The use of visible and UV dissolution imaging for the assessment of propranolol hydrochloride in liquisolid compacts of Sesamum radiatum gum

Adam Ward[a], Karl Walton[b], Slavena Stoycheva[a], Matthew Wallis[a], Adeola Adebisi[a], Elijah Nep[a, c], Ndidi C. Ngwuluka[c], Seham Shaboun[a,d], Alan M. Smith[a], Barbara R. Conway[a], Kofi Asare-Addo[a]*,

[a]Department of Pharmacy, University of Huddersfield, Huddersfield, HD1 3DH, UK

[b]EPSRC Future Metrology Hub, University of Huddersfield, Huddersfield, HD1 3DH, UK

[c]Department of Pharmaceutics and Pharmaceutical Technology, Faculty of Pharmaceutical Science, University of Jos, PMB 2084, Jos, Nigeria, 930001

[d]Pharmaceutical Chemistry Department, Faculty of Pharmacy, University of Benghazi, Libya

*Corresponding author (Kofi Asare-Addo)

e-mail: k.asare-addo@hud.ac.uk

Tel: +44 1484 472360

Fax: +44 1484 472182

Submission: JDDST

Declaration of Interest: NONE

Abstract

This work explores the first use of UV imaging in liquisolid systems. The aim of this study was to simultaneously measure a model drug propranolol hydrochloride (PPN) release and compact swelling behaviour from liquisolid systems using sesamum radiatum gum by exploiting the visible and UV imaging capabilities of the novel surface dissolution instrument (SDI2). Liquisolid compacts were successfully prepared using polysorbate 80 as the liquid solvent. The influence of either colloidal silica or veegum (magnesium aluminium silicate) was also evaluated in the liquisolid sesamum gum compacts. Solid-state characterization using differential scanning calorimetry (DSC) and X-ray powder diffraction (XRPD) showed a decrease in the crystallinity of the model cationic drug. Visible and UV imaging was successfully used to detect differences between the conventional or physical mixture formulations containing veegum or colloidal silica and the liquisolid preparations as well as differences between their swelling behaviour. The use of this imaging technique provides added insights into the drug release behaviour of formulations.

Keywords: Liquisolid; UV imaging; Propranolol; Veegum; Sesamum

Abbreviations: API, active pharmaceutical ingredients; MAS, magnesium aluminium silicate; PPN, Propranolol hydrochloride; SDI, surface dissolution imaging; IDR, Intrinsic dissolution rate; DSC, differential scanning calorimetry; XRPD, X-ray powder diffraction

Graphical abstract

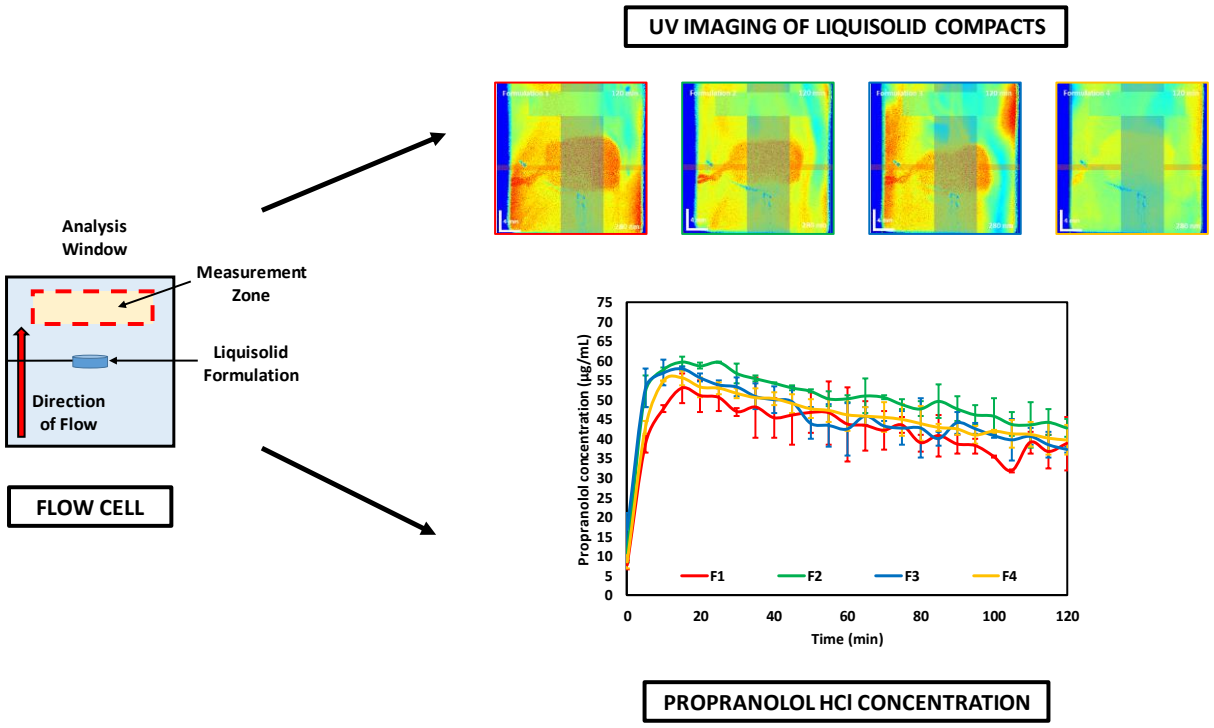

1. Introduction

Liquisolid dosage forms are an innovative way of sustaining the release of water-soluble drugs and increasing the release rate of water-insoluble drugs. Adding the liquid phase to a dry blend of excipients allows for the production of a good flowing and compactable powder to formulate the liquid-solid tablets (Spireas, Wang, & Grover, 1999). Liquisolid formulations have been utilised to restrict the release of high solubility drugs such as propranolol hydrochloride (PPN), diltiazem hydrochloride and raloxifene hydrochloride (Kaialy et al., 2016; Javadzadeh, Musaalrezaei, & Nokhodchi, 2008; Komala, Janga, Jukanti, Bandari, & Vijayagopal, 2015). Other groups have utilised liquisolid formulations in the delivery of poorly soluble drugs including candesartan, progesterone, carbamazepine and valsartan (Chella, Shastri, &

Tadikonda, 2012; Jadhav, Irny, & Patil, 2017; Javadzadeh, Jafari-Navimipour, & Nokhodchi, 2007; Sayyad, Tulsankar, & Kolap, 2013).

There is a lot of focus on naturally occurring polymers as matrix formers for oral controlled release applications. Modified release formulations offer a steady release of drug into circulation. Several authors have also investigated the complex interactions between swelling, erosion and diffusion kinetics for drug release for these natural polymers (Nokhodchi et al., 2015; Nokhodchi and Asare-Addo, 2014; Nokhodchi, Raja, Patel, & Asare-Addo, 2012; Crowley et al., 2004; Naggar et al., 1992; Bonferoni et al., 1993; Sujja-areevath et al., 1996; Talukdar et al., 1996; Khullar et al., 1998; Kaialy et al., 2013; Nep et al., 2015, 2017; Siahi-Shadbad et al., 2011; Peppas and Sahlin, 1989; Lee and Kim, 1991; Colombo et al., 1995; Reynolds et al., 1998). These renewable sources of natural polymers have greater advantages over their synthetic and semisynthetic counterparts in the developing world (Nep et al., 2016a). Here, the authors focus on a polysaccharide that has been extracted and characterised in our lab (*Sesamum radiatum*) and reported (Nep et al., 2016a). Sesamum gum is a very abundant natural polymer extracted from the leaves of *Sesamum radiatum* and has been reported for having the potential for retarding drug release from matrix systems as well as having the ability to withstand hydroalcoholic media effects (Ngwuluka, Nep, Ochekpe, Odumosu, & Olorunfemi, 2014; Nep et al., 2016; 2018). It has also been used to improve the dissolution behaviour of ibuprofen and as a binder (Shaboun et al., 2018; Allagh et al., 2005). This work explores the use of sesamum gum in liquisolid tablet formulations. The authors also investigate the use of veegum in liquisolid application. Veegum also known as magnesium aluminium silicate (MAS) is a clay mineral that has been used as a carrier for active pharmaceutical ingredients (API) in modulating their drug release (Aguzzi, Cerezo, Viseras, & Caramella, 2007; Adebisi et al., 2015; Trivedi et al., 2018) due to its inherent ability to form complexes

with cationic drugs (Totea et al., 2019a, 2019b; Pongjanyakul et al., 2005, 2007, 2009, 2011; Khlibsuwan et al., 2017, 2018).

UV dissolution imaging has begun to establish its versatility within the field of pharmaceutics. The primary use of the technique is to obtain intrinsic dissolution rates (IDR) of pharmaceutical ingredients (Boetker et al., 2013; Ward et al., 2017; Ostergaard 2018; Long et al., 2019). There has also been other applications with this technique including visualising insulin from lipid implants (Jensen et al., 2016), drug release from an in-situ forming implant (Sun et al., 2018), imaging piroxicam supersaturation, precipitation and dissolution (Sun et al., 2018a) and drug release from biodegradable microwells (Nielsen et al., 2015). This imaging technique has however begun to diversify into an analytical tool for the monitoring of a variety of dissolution events, helped in part through advancements in the technology in the form of the SDI2™ instrument manufactured by Pion Inc. This model has an added functionality to monitor whole dosage forms alongside the more traditional IDR measurements. This has allowed for capsules containing salts and solid dispersions to be imaged in real time (Asare-Addo et al., 2018; Asare-Addo et al., 2019). More recently, the technique was used to monitor the gel growth of hypromellose compacts in real time with a high level of accuracy (Ward et al., 2019). The SDI2 also has the capability of monitoring a sample with two wavelengths simultaneously. This feature is employed in the current work in the form of a 280 nm wavelength (for drug release) and 520 nm (monitoring tablet integrity). This study therefore aimed for the first time at simultaneously measuring drug release as well as compact integrity in liquisolid compacts from sesamum gum and veegum.

2. Materials and Methods

2.1. Materials

Propranolol hydrochloride (PPN) was purchased from Fischer Scientific, UK. Veegum F was a kind gift from Lake Chemicals and Minerals, UK. Polysorbate 80 was purchased from Fluka, UK. Colloidal silica was from Sigma -Aldrich. Sesamum gum was extracted from *Sesamum radiatum* leaves in-house. Potassium phosphate monobasic, sodium hydroxide and hydrochloric acid were purchased from Fischer Scientific, UK. Potassium Chloride was purchased from Sigma Aldrich, UK.

2.2. Extraction of Sesamum Gum

The extraction of sesamum gum was conducted as reported in Nep et al., 2016. In brief, 1000 g of leaves of the sesamum radiatum were macerated for 30 min at ~22 °C (in 7.5 L of distilled water containing 0.1 %w/v sodium metabisulphite). The filtered mucilage was then precipitated with 96 % ethanol, filtered again and oven dried at 50 °C for 24 h.

2.3. Preparation of formulation blends, powder flow assessment and tableting

For the liquisolid formulation, it is necessary to select an appropriate solvent to disperse the PPN in. 4 solvents were tested; Propylene Glycol, PEG 400, Glycerin and Polysorbate 80 (Javadzadeh et al., 2008). Polysorbate 80 was chosen due to PPN's low solubility in it (Javadzadeh et al., 2008).

To explore the use of imaging in liquisolid systems in comparison to its conventional counterparts, four formulations as in Table 1 were prepared. For the conventional tablets (physical mixture, F2 and F3), all the required excipients and API were mixed and blended using a Turbula™ mixer (Willy. A Bachofen, Switzerland) for 10 min before tabletting. For the liquisolid formulations (F1 and F4), 2 g of the PPN was dispersed in 2 g polysorbate 80 using a pestle and mortar for 2 min. Depending on the formulation, a dry powder blend of the sesamum gum, colloidal silica or veegum (prepared using a Turbula™ mixer (Willy. A

Bachofen, Switzerland) for 10 min) was then added to the PPN in small amounts (~500 mg) under continuous stirring until a homogenous blend was achieved.

The flow properties of all the formulations were determined using a 10 mL glass cylinder with 10 mL worth of powder from each of the formulations. The weight of the powder formulation was noted each time and then the glass cylinder tapped to allow the particles of powder to consolidate. After 50 taps, the final volume was recorded. Carr's consolidation index was determined using Equation 1.

$$Carr's\ Index = 100\ x\ (\frac{1-Bulk\ Density}{Tapped\ Density}) \qquad \text{Equation 1}$$

For the tablet manufacture, round cylindrical tablets with a diameter of 10 mm and target weights of 285 mg (conventional of physical mixture) or 400 mg (liquisolid compacts) were compacted using a manual single punch hydraulic press at 2500 psi in a 10 mm punch and die (Model MTCM-1, Globe Pharma, US) at 2500 psi.

2.4. Tablet friability and hardness testing

Friability testing was carried out on 10 tablets for each formulation using a Pharmatest Friability tester. The tablets were firstly dusted gently using a brush in order to remove any powder debris and then weighed. The tablets were then dusted again after being subjected to 25 rpm for 4 min, dusted off and re-weighed to measure any loss in weight. Friability (%) was determined using Equation 2.

$$\left(\frac{Initial\ weight\ of\ 10\ tablets\ (g) - weight\ of\ 10\ tablets\ after\ 100\ spins\ (g)}{Initial\ weight\ of\ 10\ tablets\ (g)}\right)\ X\ 100 = Friability\ of\ tablets\ (\%) \qquad \text{Equation 2}$$

Tablets from each formulation were allowed at least 24 h recovery time before being subjected to the Pharmatest hardness tester to determine breaking force. The point at which the tablet fractured was recorded in Newtons (N).

2.5. Solid state characterisation

2.5.1. Differential scanning calorimetry (DSC)

Approximately 3.5 mg of each formulation was placed in a standard aluminium pan (40 µL) with a vented lid. This was then crimped and heated from 30 to 300 °C at a scanning rate of 10 °C/min with nitrogen gas as the purge gas (DSC1 Mettler-Toledo, Switzerland). The enthalpy, onset temperatures and melting points of the starting materials and the various formulation were analysed using the software provided by Mettler-Toledo, Switzerland.

2.5.2. X-ray powder diffraction (XRPD)

The XRPD patterns of each formulation as well as their starting materials were scanned in Bragg–Brentano geometry, over a scattering (Bragg, 2θ) angle range from 5 to 45°, in 0.02° steps at 1.5° min^{-1} using a D2 Phaser diffractometer (Bruker AXS GmbH, Karlsruhe, Germany) (Laity et al., 2015). Microsoft Excel was used to analyze the collected XRPD patterns.

2.6. UV imaging and dissolution of whole dosage form

2.6.1 Calibration of the SDI2 system

This work tested a novel method of utilising the SDI2 system (Pion Inc. USA) in performing the UV calibration of the PPN by utilizing the systems own whole dosage cell. This allowed for the imaging of PPN from the conventional and liquisolid compacts. Two stock solutions were prepared to a concentration of 1 mg/mL and labelled A and B using pH 6.8 phosphate

buffer. Standards were prepared from both stocks with a concentration ranging from 100 µg/mL to 1 µg/mL.

Next, the whole dosage cell (absent of glass beads) was inserted into the SDI2. Using the data collection software supplied, a method was devised to record each standard at the selected wavelength of 280 nm for 10 min with a 5 min gap to allow for change of standard. The system was blanked with pH 6.8 phosphate buffer and each standard was tested in increasing order starting with 1 µg/mL. Figure 1a highlights how the measurement of absorbance from the images was taken from the SDI2 system. The recorded data was further analysed using the supplied analysis software and the calibration curve plotted using Microsoft Excel to allow the determination of the extinction coefficient (Figure 1b). Figure 1c depicts the absorbance images produced from the varying PPN concentration used for the calibration curve (R^2 value = 0.9872).

2.6.2 UV Imaging and Dissolution

A schematic of how the formulations were tested and analysed utilising the whole dosage flow cell is indicated in Figure 2. Figure 2 also displays how the dosage form is placed inside the whole dose cell, the direction of media (pH 6.8 phosphate buffer) flow and the measurement zone adopted for PPN evaluation. Conventional or liquisolid compacts were mounted using a stainless-steel wire holder and placed within the sample cell (Figure 2). The whole dosage cell with glass beads loaded (to help reduce turbulence) was inserted and connected to the fluid lines. The experiment was conducted using pH 6.8 phosphate buffer at a flow rate of 8.2 mL/min at 37 °C. The release of PPN was imaged over 120 min at various time points at a wavelength of 280 nm. Drug release profiles and cumulative percentage release profiles were determined from the absorbance data from the SDI2 system using the calibration curve equation generated from Figure 1b and the equations 3 and 4 described:

196 a) $mass\ (mg) = \frac{Concentration \times 68\ mL}{1000}$ Equation 3

197 b) $Release\ (\%) = \left(\frac{mass}{dose}\right) \times 100$ Equation 4

198 The concentration was measured in µg/mL as per the calibration curve. Cumulative amount
199 was calculated as the sum total at each subsequent time point. It is important to note that the
200 volume of 68 mL is the manufacturer stated volume of the whole dosage cell, therefore this
201 was used to calculate the amount of drug released from the liquisolid compacts. The dose of
202 propranolol hydrochloride in all the manufactured compacts was 114 mg. Tablet growth
203 measurements were also taken using the 520 nm LED. Growth measurements are expressed as
204 a percentage of the starting size of the tablet.

205 **3. RESULTS AND DISCUSSION**

206 **3.1. Solid-state analysis of starting materials and formulations**

207 The sesamum gum was successfully extracted and characterised. The gums characterisation
208 has been extensively reported elsewhere (Nep et al., 2016, 2016a, 2018). In brief, sesamum is
209 an amorphous polymer (Figure 3a). PPN displays distinctive characteristic peaks at 2theta
210 angles of; 12.51°, 16.73°, 17.19°, 19.76°, 23.22°, 25.08° and 27.47° (indicated by red stars on
211 Figure 3a) (Bartolomei, Bertocchi, Ramusino, Santucci, & Valvo, 1999). XRPD showed the
212 colloidal silica to also be amorphous. The XRPD pattern for the veegum showed that the
213 majority of the reflections are quite broad which is consistent with small or distorted crystallites
214 (Figure 3a) (Laity et al., 2015).

215 DSC highlighted PPN to have a sharp endothermic peak with an onset of 163.1 °C, a melt at
216 165.8 °C (indicated by the red arrow) and an enthalpy of 271.8 mJ. The melt was consistent
217 with data reported by Javadzadeh et al. 2008. The colloidal silica was shown to be amorphous
218 in the DSC thermographs (Figure 3b). The thermal behaviour of sesamum has been reported

by Nep et al. 2018. The authors observed minor weight loss of ~ 11.5 % between 50 -140 °C using TGA analysis and DSC. This was attributed to the loss of water (adsorbed and structural water) or desorption of moisture from the polysaccharide structure (Nep 2018; Vendruscolo et al., 2009; Iqbal et al., 2011). The other event on the sesamum DSC trace is attributed to the polysaccharide decomposition (Zohuriaan and Shokrolahi 2004; Varma et al., 1997) between 251 and 302.3 °C. This phenomenon was confirmed using TGA analysis as a final weight loss of ~ 54.6 % by Nep et al. 2018 with the thermal scission of carboxylate or carboxylic acid groups resulting in the evolution of $C0_2$ from the corresponding carbohydrate backbone being a probable mechanism for the observations.

Figure 3c highlights that the characteristic peaks of PPN was present in all formulations (conventional and liquisolid). Interestingly, no significant differences in the diffraction pattern was noticed between the liquisolid formulations and their physical mixtures although F1 seemed to be the most crystalline. The DSC results (Figure 3d) showed that all formulations tested displayed the endothermic peak for PPN (F1: onset temperature of 160 °C, melt peak of 164.7 °C and enthalpy of 72.9 mJ, F2: onset temperature of 160.7 °C, melt peak of 163.5 °C and enthalpy of 16.93 mJ, F3: onset temperature of 160.6 °C, melt peak of 163.9 °C and enthalpy of 22.46 mJ and F4: onset temperature of 157.3 °C, melt peak of 163.2 °C and enthalpy of 37.3 mJ). The significant decrease in enthalpy of melt corresponds to the decrease in crystallinity as also observed in Figure 3c.

3.2. Tablet Characterization

The conventional and liquisolid formulations tested displayed a Carr's consolidation index of 27 to 32 indicating poor flowability. Both the physical mixtures (F2 and F3) displayed greater tablet hardness (207.90 ± 5.88 and 248.10 ± 20.59 N respectively) than the liquisolid

formulations F1 and F4 (15.98 ± 1.96 and 8.14 ± 1.96 N respectively). This is attributed to the introduction of the liquid vehicle polysorbate 80 into the liquisolid compacts. It was also noted that the presence of veegum in place of the colloidal silica inferred further hardness to the conventional compacts. Laity et al., 2015 reported veegum to make hard compacts. Interestingly, the formulations containing colloidal silica (F1 and F2) had friability values of 0.5 % whereas the formulations containing veegum did not have any friability issues. Figure 4 provides a visual assessment of how the formulations looked post tabletting. It appeared that the physical or conventional compact (F2 and F3) experienced a large amount of mottling, indicated by the red arrows. This could be due in part to the differing particle sizes of the colloidal silica, PPN present and sesamum gum present. This may have also caused segregation issues. The liquisolid compact were however very uniform looking due to their preparation method.

3.3. Dissolution Study

UV imaging systems are known to have limited linear ranges. This was experienced during the calibration of the whole dose system in determining the release of PPN from the produced compacts. The calibration curve allowed for measurements of up to 1100 mAU. Some of the images from Figure 5 therefore indicates a limitation of the instrumentation as there was a saturation of the detector with PPN (up to 2000 mAU for the snapshot UV images taken). This implies further differences between the formulations may therefore be minimised. The saturation of the detector up to the 30 min time point can be attributed the drug coming off the surfaces of the compact before initial gel formation to control drug release. This can also be viewed as the initial burst release that can be experienced by hydrophilic matrices formulated with very soluble drugs (Javadzadeh et al., 2008). It is also important to note that the r^2 value obtained for the calibration was 0.9872 which suggests a deviation from linearity for the SDI instrument. This suggests that there might be a degree of error with quantitative analysis. The

SDI2 dissolution imaging system was used to perform all dissolution studies in this work. Figure 5 a-b, displays the images recorded for the formulations containing colloidal silica. The images appears to show qualitatively that initially, the physical mixture (F2) released a greater amount of the drug between 1 and 30 min when compared to its liquisolid formulation counterpart (F1). The deviation in linearity makes it difficult to view the data in a quantitative way (Figure 6a) however, a comparison of the cumulative release profile (Figure 6b) using the obtained calibration curve indicates that at 60 min, F2 released an average of approximately 468 µg/mL compared to an average of 361 µg/mL from the F1 compacts. This result is supported by work completed by Javadzadeh et al., 2007 where the authors utilised polysorbate in liquisolid formulations to delay the dissolution rate from tablet matrices. It is important to however note that overlap of some of the standard deviations suggests that these may be similar. The images also displayed a greater level of hydration and swelling in the liquisolid formulation (F1) indicated by the greater tablet size (normalised and plotted in Figure 6c). This may well have contributed to the lower drug release from the liquisolid compacts as the diffusion length for the drug diffusion would have increased as a result. The ability of UV imaging to visualise hydration and drug release simultaneously gives a unique insight in to the dissolution process when compared to conventional non-imaging dissolution systems.

Figure 7 displays the images recorded from the formulations containing veegum. From the images it appears that both the physical mixture (F3) and the liquisolid formulation (F4) do not seem distinctly different although F3 seems to have slightly more intense absorbance than F4. This was further supported by the profiles displayed in Figure 6a. Both the dissolution profiles are very similar suggesting that the concentration of veegum used here was not as effective as the colloidal silica at the same concentration (F1 and F2). Another interesting observation from the images in Figure 6b was that after normalising tablet growth, the physical or conventional

formulation compact F3 hydrated to a greater size during dissolution than its liquisolid compact F4 (Figure 6c).

4. Conclusion

The presented work successfully formulated liquisolid dosage forms using a sesamum gum. This work demonstrated that dissolution imaging can be used effectively in determining drug release from liquisolid systems and providing a crucial visual aid to the formulator. This work also explored the incorporation of the clay composite veegum into formulation of liquisolid systems. Veegum was successfully incorporated into the liquisolid tablet as a substitute for the colloidal silica at the ratio tested. UV imaging therefore presents a platform that can provide insights into various dosage forms.

5. Acknowledgements

The authors would like to acknowledge the University of Huddersfield for financial support.

6. References

Adebisi, A. O., Conway, B. R., & Asare-Addo, K. (2015). The influence of fillers on theophylline release from clay matrices. *American Journal of Pharmacological Sciences*, *3*(5), 120-125.

Aguzzi, C., Cerezo, P., Viseras, C., & Caramella, C. (2007). Use of clays as drug delivery systems: Possibilities and limitations. *Applied Clay Science, 36*(1-3), 22-36.

Allagh, T.S., Meseke, A., Ibrahim, Y.K.E. (2005). Evaluation of the tablet binding properties of *Sesamum radiatum*. *Nig J Pharm Res* 4 (1), 46 – 50.

313 Asare-Addo, K., Alshafiee, M., Walton, K., Ward, A., Totea, A., Taheri, S., . . . Conway, B.
314 R. (2019). *Effect of preparation method on the surface properties and UV imaging of*
315 *indomethacin solid dispersions* doi://doi.org/10.1016/j.ejpb.2019.03.002

316 Asare-Addo, K., Walton, K., Ward, A., Totea, A., Taheri, S., Alshafiee, M., Mawla, N.,
317 Bondi, A., Evans, W., Adebisi, A., Conway B.R and Timmins, P. (2018). *Direct imaging*
318 *of the dissolution of salt forms of a carboxylic acid drug International Journal of*
319 *Pharmaceutics, 551*(1-2), 290-299. doi://doi.org/10.1016/j.ijpharm.2018.09.048

320 Bartolomei, M., Bertocchi, P., Ramusino, M. C., Santucci, N., & Valvo, L. (1999). Physico-
321 chemical characterisation of the modifications I and II of (R, S) propranolol
322 hydrochloride: Solubility and dissolution studies. *Journal of Pharmaceutical and*
323 *Biomedical Analysis, 21*(2), 299-309.

324 Boetker, J. P., Rantanen, J., Rades, T., Müllertz, A., Østergaard, J., & Jensen, H. (2013). A
325 new approach to dissolution testing by UV imaging and finite element simulations.
326 *Pharmaceutical Research, 30*(5), 1328-1337. doi:10.1007/s11095-013-0972-0

327 Bonferoni, M.C., Rossi, S., Tamayo, M., Pedraz, J.L., Dominguez-Gil, A., Caramella, C.,
328 (1993). On the employment of l-carrageenan in a matrix system. I. Sensitivity to
329 dissolution medium and comparison with Na carboxymethylcellulose and xanthan gum.
330 *J. Control. Release* 26, 119–127.

331 Chella, N., Shastri, N., & Tadikonda, R. R. (2012). *Use of the liquisolid compact technique*
332 *for improvement of the dissolution rate of valsartan*
333 doi://doi.org/10.1016/j.apsb.2012.07.005

Colombo, P., Bettini, R., Massimo, G., Catellani, P.L., Santi, P., Peppas, N.A. (1995). Drug diffusion front movement is important in drug release control from swellable matrix tablets. *J. Pharm. Sci*. 84 (8), 991–997.

Crowley, M. M., Schroeder, B., Fredersdorf, A., Obara, S., Talarico, M., Kucera, S., & McGinity, J. W. (2004). Physicochemical properties and mechanism of drug release from ethyl cellulose matrix tablets prepared by direct compression and hot-melt extrusion. *International Journal of Pharmaceutics, 269*(2), 509-522.

Iqbal MS, Akbar J, Saghir S, et al. Thermal studies of plant carbohydrate polymer hydrogels. Carbohydr. Polym. [Internet]. 2011;86:1775–1783. Available from: http://www.sciencedirect.com/science/article/pii/S0144861711005960.

Jadhav, N. R., Irny, P. V., & Patil, U. S. (2017). *Solid state behavior of progesterone and its release from neusilin US2 based liquisolid compacts* doi://doi.org/10.1016/j.jddst.2017.01.009

Javadzadeh, Y., Jafari-Navimipour, B., & Nokhodchi, A. (2007). *Liquisolid technique for dissolution rate enhancement of a high dose water-insoluble drug (carbamazepine)* doi://doi.org/10.1016/j.ijpharm.2007.03.034

Javadzadeh, Y., Musaalrezaei, L., & Nokhodchi, A. (2008). *Liquisolid technique as a new approach to sustain propranolol hydrochloride release from tablet matrices* doi://doi.org/10.1016/j.ijpharm.2008.06.022

Jensen, S. S., Jensen, H., Møller, E. H., Cornett, C., Siepmann, F., Siepmann, J., & Østergaard, J. (2016). In vitro release studies of insulin from lipid implants in solution

and in a hydrogel matrix mimicking the subcutis. *European journal of pharmaceutical sciences*, *81*, 103-112.

Kaialy W, Emami P, Asare-Addo K, Shojaee S, Nokhodchi A. (2013). Psyllium: a promising polymer for sustained release formulations in combination with HPMC polymers. *Pharm Dev Technol*, 2014; 19 (3):269–277

Kaialy, W., Bello, H., Asare-Addo, K., & Nokhodchi, A. (2016). Effect of solvent on retarding the release of diltiazem HC l from Polyox-based liquisolid tablets. *Journal of Pharmacy and Pharmacology*, *68*(11), 1396-1402.

Khlibsuwan, R., Siepmann, F., Siepmann, J., & Pongjanyakul, T. (2017). Chitosan-clay nanocomposite microparticles for controlled drug delivery: Effects of the MAS content and TPP crosslinking. *Journal of Drug Delivery Science and Technology*, *40*, 1-10.

Khlibsuwan, R., Tansena, W., & Pongjanyakul, T. (2018). Modification of alginate beads using gelatinized and ungelatinized arrowroot (Tacca leontopetaloides L. Kuntze) starch for drug delivery. *International journal of biological macromolecules*, *118*, 683-692.

Komala, D. R., Janga, K. Y., Jukanti, R., Bandari, S., & Vijayagopal, M. (2015). *Competence of raloxifene hydrochloride loaded liquisolid compacts for improved dissolution and intestinal permeation* doi://doi.org/10.1016/j.jddst.2015.10.020

Khullar, P., Khar, R.K., Agarwal, S.P., (1998). Evaluation of guar gum in the preparation of sustained-release matrix tablets. *Drug Dev. Ind. Pharm*. 24 (11), 1095–1099.

Lee, P.I., Kim, C.J. (1991). Probing the mechanisms of drug release from hydrogels. *J. Control. Release*, 16, 229–236

376 Long, C. M., Tang, K., Chokshi, H., & Fotaki, N. (2019). Surface Dissolution UV Imaging
377 for Investigation of Dissolution of Poorly Soluble Drugs and Their Amorphous
378 Formulation. *AAPS PharmSciTech*, *20*(3), 113.

379 Naggar, V.F., El-Khawas, M., Ismail, F.A., Boraie, N.A. (1992). Pectin, a possible matrix for
380 oral sustained-release preparations of water-soluble drugs. *STP Pharma. Sci*. 2 (3), 227–
381 234.

382 Nep, E., Asare-Addo, K., Ngwuluka, N., Conway, B. R., & Smith, A. M. (2016). Evaluation
383 of sesamum gum as an excipient in matrix tablets. *British Journal of Pharmacy*, *1*(1).

384 Nep, E. I., Asare-Addo, K., Ghori, M. U., Conway, B. R., & Smith, A. M. (2015). Starch-free
385 grewia gum matrices: Compaction, swelling, erosion and drug release behaviour.
386 *International journal of pharmaceutics*, *496*(2), 689-698.

387 Nep, E. I., Mahdi, M. H., Adebisi, A. O., Dawson, C., Walton, K., Bills, P. J., ... & Asare-
388 Addo, K. (2017). The influence of hydroalcoholic media on the performance of Grewia
389 polysaccharide in sustained release tablets. *International journal of pharmaceutics*,
390 *532*(1), 352-364.

391 Nep, E. I., Mahdi, M. H., Adebisi, A. O., Ngwuluka, N. C., Conway, B. R., Smith, A. M., &
392 Asare-Addo, K. (2018). Hydro-alcoholic media effects on theophylline release from
393 sesamum polysaccharide gum matrices. *Drug development and industrial pharmacy*,
394 *44*(2), 251-260.

395 Nep, E. I., Carnachan, S. M., Ngwuluka, N. C., Kontogiorgos, V., Morris, G. A., Sims, I. M.,
396 & Smith, A. M. (2016a). Structural characterisation and rheological properties of a

polysaccharide from sesame leaves (Sesamum radiatum Schumach. & Thonn.). *Carbohydrate polymers*, *152*, 541-547.

Nielsen, L. H., Nagstrup, J., Gordon, S., Keller, S. S., Østergaard, J., Rades, T., ... & Boisen, A. (2015). pH-triggered drug release from biodegradable microwells for oral drug delivery. *Biomedical microdevices*, *17*(3), 55.

Ngwuluka, N., Nep, E., Ochekpe, N., Odumosu, P., & Olorunfemi, P. (2014). (2014). Comparative rheological characterization of two natural polymers from sesamum radiatum and bombax buonopozense for application in drug delivery. Paper presented at the *Macromolecular Symposia, , 345*(1) 51-58.

Nokhodchi, A., & Asare-Addo, K. (2014). Drug release from matrix tablets: physiological parameters and the effect of food. *Expert opinion on drug delivery*, *11*(9), 1401-1418.

Nokhodchi, A., Palmer, D., Asare-Addo, K., Levina, M., & Rajabi-Siahboomi, A. (2015). Application of polymer combinations in extended release hydrophilic matrices. *Handbook of Polymers for Pharmaceutical Technologies*, *1*, 23-49.

Nokhodchi, A., Raja, S., Patel, P., & Asare-Addo, K. (2012). The role of oral controlled release matrix tablets in drug delivery systems. *BioImpacts: BI*, *2*(4), 175.

Østergaard, J. (2018). UV imaging in pharmaceutical analysis. *Journal of pharmaceutical and biomedical analysis*, *147*, 140-148.

Peppas, N.A., Sahlin, J.J. (1989). A simple equation for the description of solute release. III. Coupling of diffusion and relaxation. *Int. J. Pharm*, 57, 169–172.

417 Pongjanyakul, T., & Suksri, H. (2009). Alginate-magnesium aluminum silicate films for
418 buccal delivery of nicotine. *Colloids and Surfaces B: Biointerfaces, 74*(1), 103-113.

419 Pongjanyakul, T., & Puttipipatkhachorn, S. (2007). Xanthan–alginate composite gel beads:
420 molecular interaction and in vitro characterization. *International Journal of*
421 *Pharmaceutics, 331*(1), 61-71.

422 Pongjanyakul, T., Priprem, A., & Puttipipatkhachorn, S. (2005). Investigation of novel
423 alginate− magnesium aluminum silicate microcomposite films for modified-release
424 tablets. *Journal of controlled release, 107*(2), 343-356.

425 Khunawattanakul, W., Puttipipatkhachorn, S., Rades, T., & Pongjanyakul, T. (2011). Novel
426 chitosan− magnesium aluminum silicate nanocomposite film coatings for modified-
427 release tablets. *International journal of pharmaceutics, 407*(1-2), 132-141.

428 Reynolds, T.D., Gehrke, S.H., Hussain, A.S., Shenouda, L.S. (1998). Polymer erosion and
429 drug release characterisation of hydroxypropylmethylcellulose matrices. *J. Pharm. Sci,*
430 87 (9), 1115–1123.

431 Rojtanatanya, S., & Pongjanyakul, T. (2010). *Propranolol–magnesium aluminum silicate*
432 *complex dispersions and particles: Characterization and factors influencing drug*
433 *release* doi://doi.org/10.1016/j.ijpharm.2009.09.016

434 Sayyad, F. J., Tulsankar, S. L., & Kolap, U. B. (2013). *Design and development of liquisolid*
435 *compact of candesartan cilexetil to enhance dissolution*
436 doi://doi.org/10.1016/j.jopr.2013.05.012

437 Shaboun, S., Nep, E., Ngwuluka, N. C., Adebisi, A., Conway, B., Smith, A., & Asare-Addo,
438 K. (2018). Solid state and dissolution behaviour of a low melting point drug in co-milled
439 mixtures of Sesamum radiatum gum. *British Journal of Pharmacy*, *3*(1).

440 Siahi-Shadbad, M. R., Asare-Addo, K., Azizian, K., Hassanzadeh, D. & Nokhodchi, A.
441 (2011). Release behaviour of propranolol HCl from hydrophilic matrix tablets containing
442 psyllium powder in combination with hydrophilic polymers. *AAPS PharmSciTech*,
443 12(4), 1176-1182.

444 Spireas, S., Wang, T., & Grover, R. (1999). Effect of powder substrate on the dissolution
445 properties of methyclothiazide liquisolid compacts. *Drug Development and Industrial*
446 *Pharmacy*, *25*(2), 163-168.

447 Sujja-areevath, J., Munday, D.L., Cox, P.J., Khan, K.A. (1996). Release characteristics of
448 diclofenac sodium from encapsulated natural gum mini-matrix formulations. *Int. J.*
449 *Pharm*, 139, 53–62.

450 Sun, Y., Jensen, H., Petersen, N. J., Larsen, S. W., & Østergaard, J. (2018). Concomitant
451 monitoring of implant formation and drug release of in situ forming poly (lactide-co-
452 glycolide acid) implants in a hydrogel matrix mimicking the subcutis using UV–vis
453 imaging. *Journal of pharmaceutical and biomedical analysis*, *150*, 95-106.

454 Sun, Y., Chapman, A., Larsen, S. W., Jensen, H., Petersen, N. J., Goodall, D. M., &
455 Østergaard, J. (2018a). UV–vis Imaging of Piroxicam Supersaturation, Precipitation, and
456 Dissolution in a Flow-Through Setup. *Analytical chemistry*, *90*(11), 6413-6418.

457 Talukdar, M.M., Michoel, A., Rombaut, P., Kinget, R. (1996). Comparative study on xanthan
458 gum and hydroxypropylmethylcellulose as matrices for controlled-release drug delivery.
459 I. Compaction and in vitro drug release behaviour. *Int. J. Pharm*, 129, 233–241.

460 Totea, A. M., Dorin, I., Gavrilov, G., Laity, P. R., Conway, B. R., Waters, L., & Asare-Addo,
461 K. (2019). *Real time calorimetric characterisation of clay – drug complex dispersions*
462 *and particles* doi://doi.org/10.1016/j.ijpx.2018.100003

463 Totea, A. M., Sabin, J., Dorin, I., Hemming, K., Laity, P. R., Conway, B. R., Waters., L &
464 Asare-Addo, K. (2019). Thermodynamics of clay–Drug complex dispersions: Isothermal
465 titration calorimetry and high-performance liquid chromatography. *Journal of*
466 *Pharmaceutical Analysis*. doi://doi.org/10.1016/j.jpha.2019.12.001

467 Trivedi, V., Nandi, U., Maniruzzaman, M., & Coleman, N. J. (2018). Intercalated
468 theophylline-smectite hybrid for pH-mediated delivery. *Drug delivery and translational*
469 *research*, 1-9.

470 Varma AJ, Kokane SP, Pathak G, et al. Thermal behavior of galactomannan guar gum and its
471 periodate oxidation products. Carbohydr. Polym. [Internet]. 1997;32:111–114. Available
472 from: http://www.sciencedirect.com/science/article/pii/S0144861796001555.

473 Vendruscolo CW, Ferrero C, Pineda EAG, et al. Physicochemical and mechanical
474 characterization of galactomannan from Mimosa scabrella: Effect of drying method.
475 Carbohydr. Polym. [Internet]. 2009;76:86–93. Available from
476 http://www.sciencedirect.com/science/article/pii/S0144861708004475.

477 Ward, A., Walton, K., Box, K., Østergaard, J., Gillie, L. J., Conway, B. R., & Asare-Addo, K.
478 (2017). *Variable-focus microscopy and UV surface dissolution imaging as*

complementary techniques in intrinsic dissolution rate determination
doi://doi.org/10.1016/j.ijpharm.2017.07.053

Ward, A., Walton, K., Mawla, N., Kaialy, W., Liu, L., Timmins, P., . . . Asare-Addo, K. (2019). *Development of a novel method utilising dissolution imaging for the measurement of swelling behaviour in hydrophilic matrices*
doi://doi.org/10.1016/j.ijpx.2019.100013

Zohuriaan MJ, Shokrolahi F. Thermal studies on natural and modified gums. Polym. Test. [Internet]. 2004;23:575–579. Available from: http://www.sciencedirect.com/science/article/pii/S0142941803001648.

Tables

Table 1. Formulation components for the conventional and liquisolid compacts.

Formulation code	Propranolol hydrochloride (g)	Sesamum Gum (g)	Polysorbate 80 (g)	Colloidal Silica (g)	Veegum (g)
F1	2	2.727	2	0.273	-
F2	2	2.727	-	0.273	-
F3	2	2.727	-	-	0.273
F4	2	2.727	2	-	0.273

Figure captions

Figure 1. A schematic representation of the analysis of the calibration standards using the SDI2 whole dosage cell (a), calibration curve for propranolol hydrochloride using the SDI2 (b), associated UV images from the calibration curves (c). Wavelength used for UV analysis was 280 nm.

Figure 2. A schematic representation of the analysis of a tablet dosage form in the SDI2 whole dosage cell showing measurement zones, direction of media flow and compact orientation.

Figure 3. XRPD analysis of (a) propranolol hydrochloride, colloidal silica, sesamum gum and veegum, (b) DSC thermograms of propranolol hydrochloride, colloidal silica, sesamum gum and veegum, (c) XRPD of propranolol hydrochloride in comparison to conventional and liquisolid formulations (F1-F4), (d) DSC of propranolol hydrochloride in comparison to conventional and liquisolid formulations (F1-F4).

Figure 4. Photographs of formulations (F1-F4) post tabletting indicating some differences in tablet appearance as a result of its preparation method.

Figure 5. UV images (up to 120 min) obtained from the surface dissolution imaging instrument for a) formulation 1 (F1-liquisolid), b) formulation 2 (F2-convential or physical mixture). Wavelength used for UV analysis was 280 nm.

Figure 6. Drug release from formulations (F1-4) from the surface dissolution instrument (SDI2) (a), cumulative drug release formulations (F1-F4) from the SDI instrument (b), tablet growth profiles for formulations (F1-4) measured using the bespoke software from the SDI2 instrument (c).

Figure 7. UV images (up to 120 min) obtained from the surface dissolution imaging instrument for a) formulation 3 (F3-convential or physical mixture), b) formulation 4 (F4-liquisolid). Wavelength used for UV analysis was 280 nm.

Figures

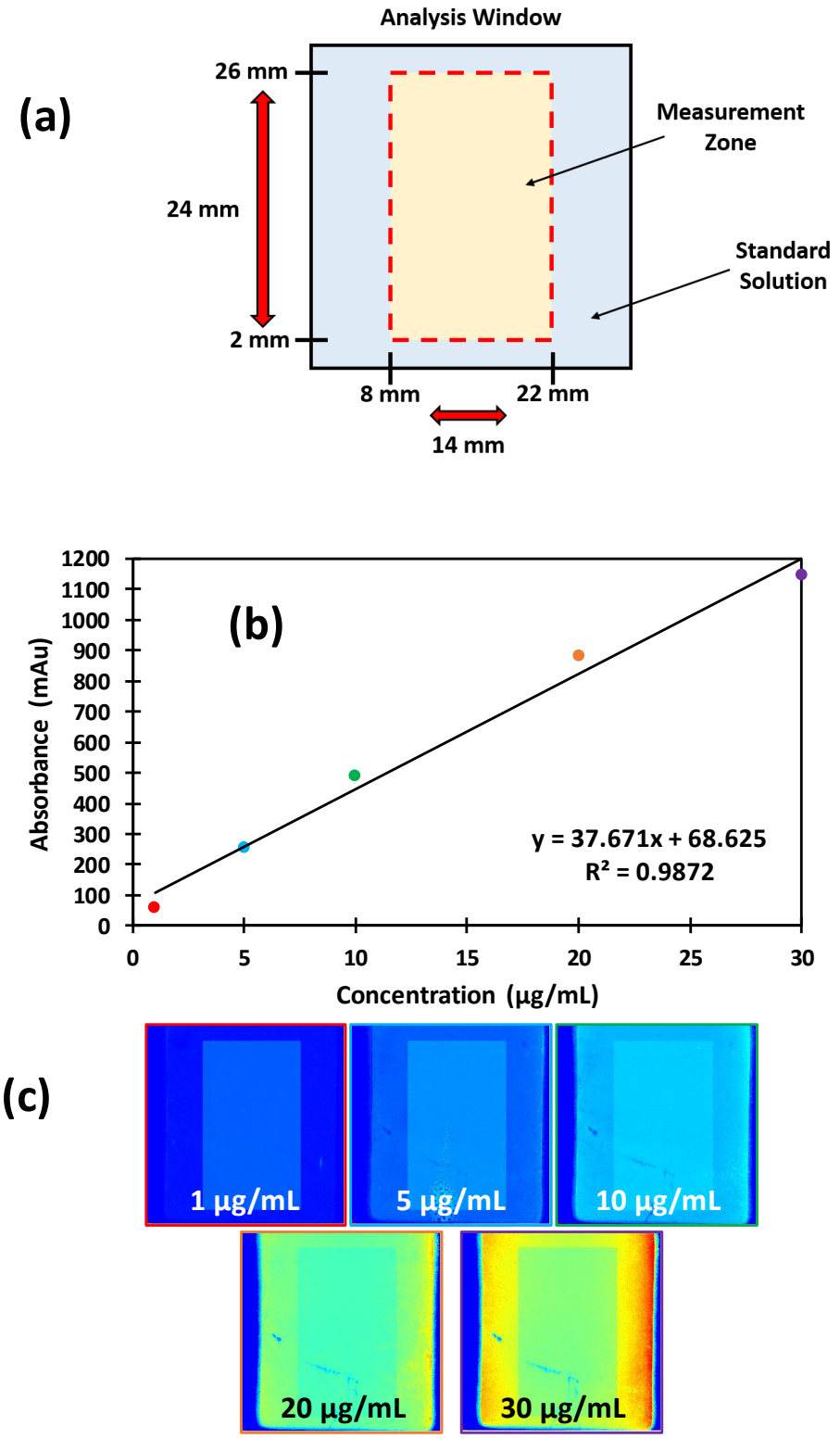

Figure 1

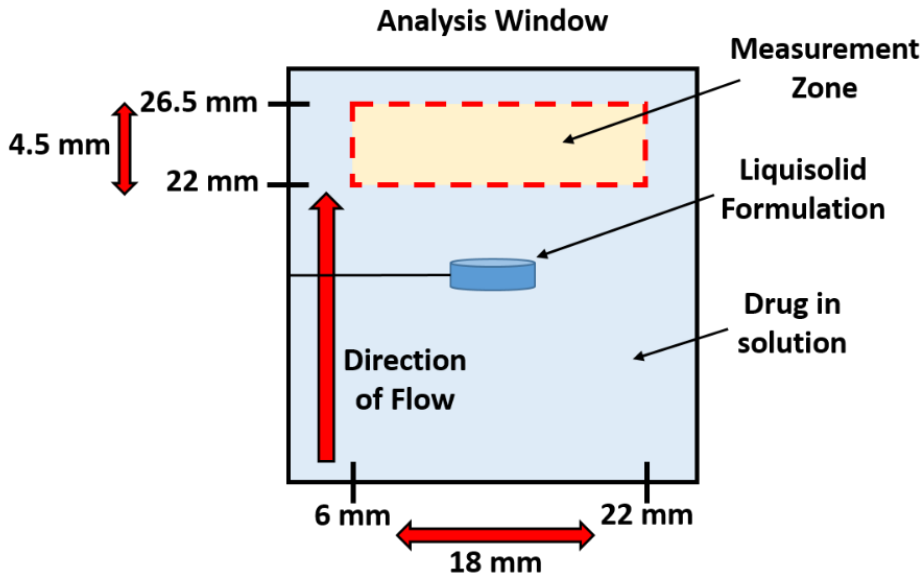

564

565

566

567 **Figure 2**

568

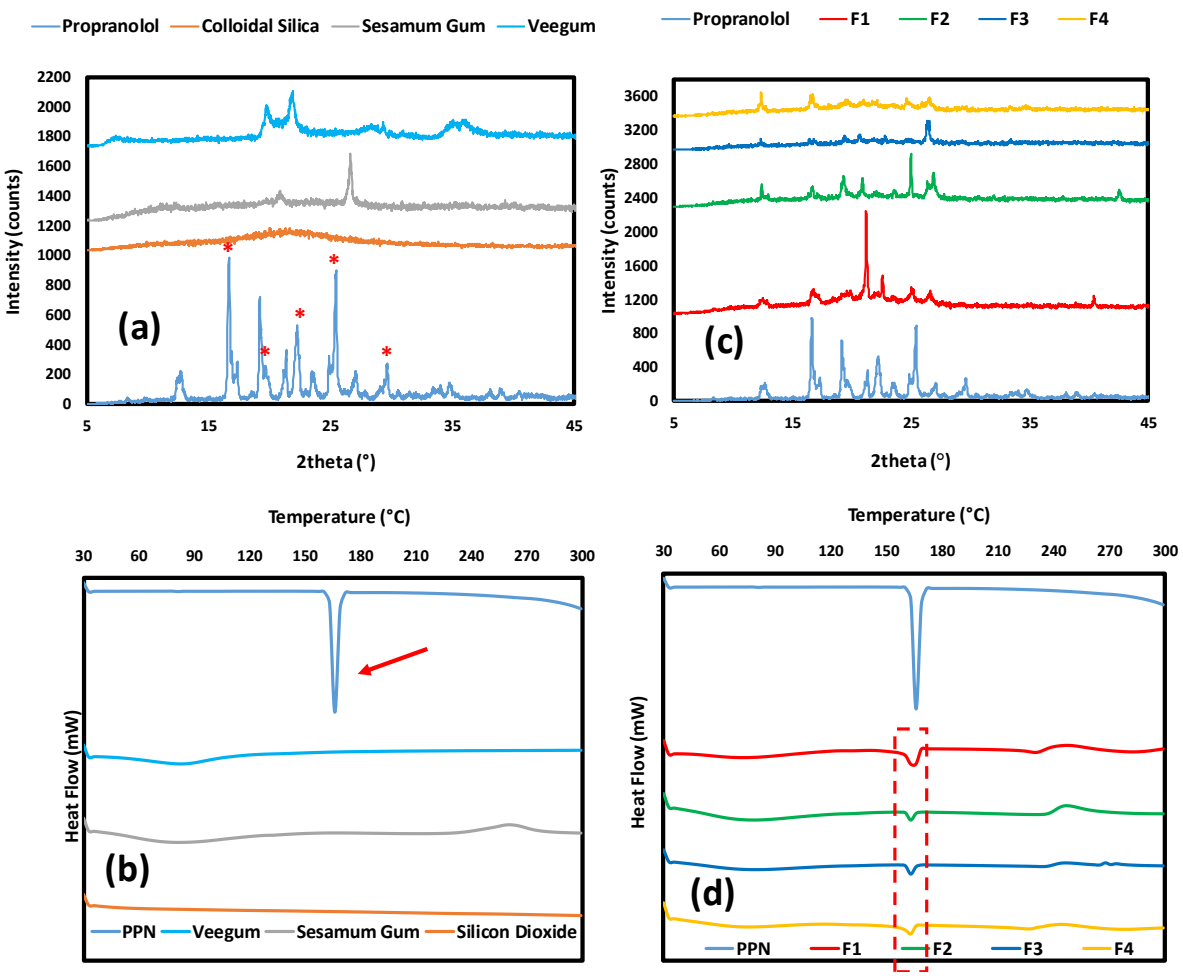
Propranolol
Colloidal Silica
Sesamum Gum
Veegum
Intensity (counts)
2theta (°)
(a)
Propranolol
F1
F2
F3
F4
Intensity (counts)
2theta (°)
(c)
Temperature (°C)
Heat Flow (mW)
(b)
PPN
Veegum
Sesamum Gum
Silicon Dioxide
Temperature (°C)
Heat Flow (mW)
(d)
PPN
F1
F2
F3
F4

Figure 3

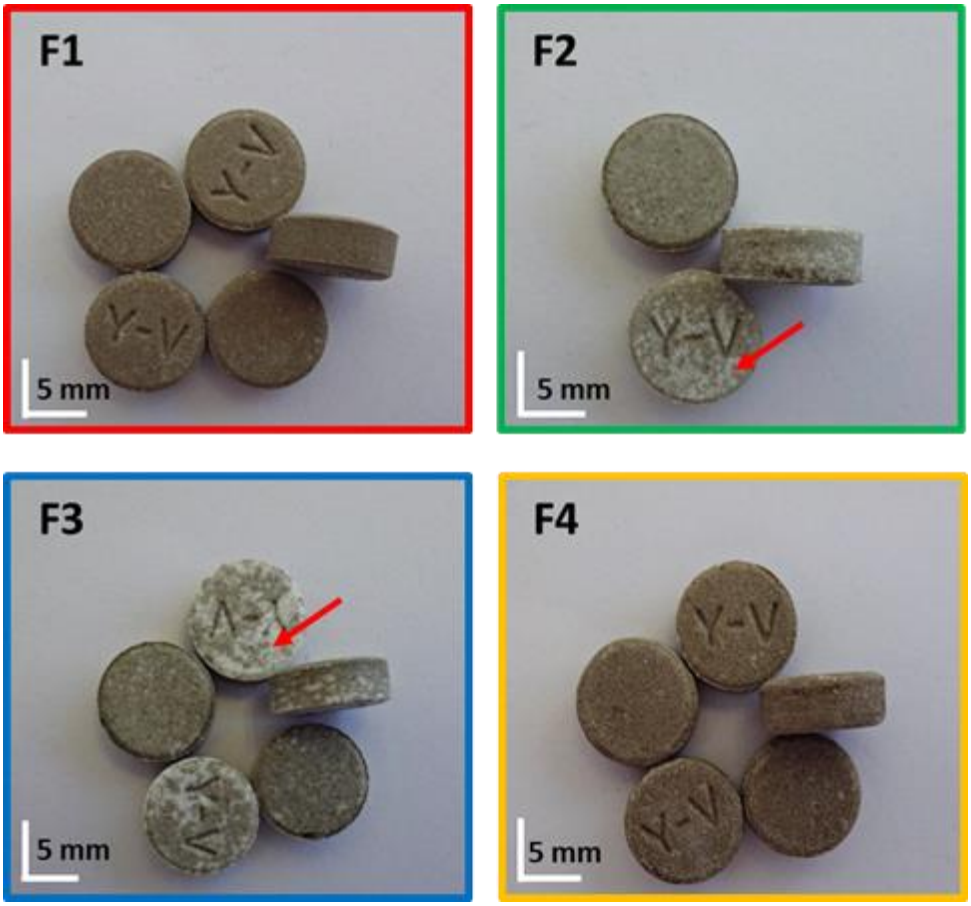

574

575

576

577 **Figure 4**

578

579

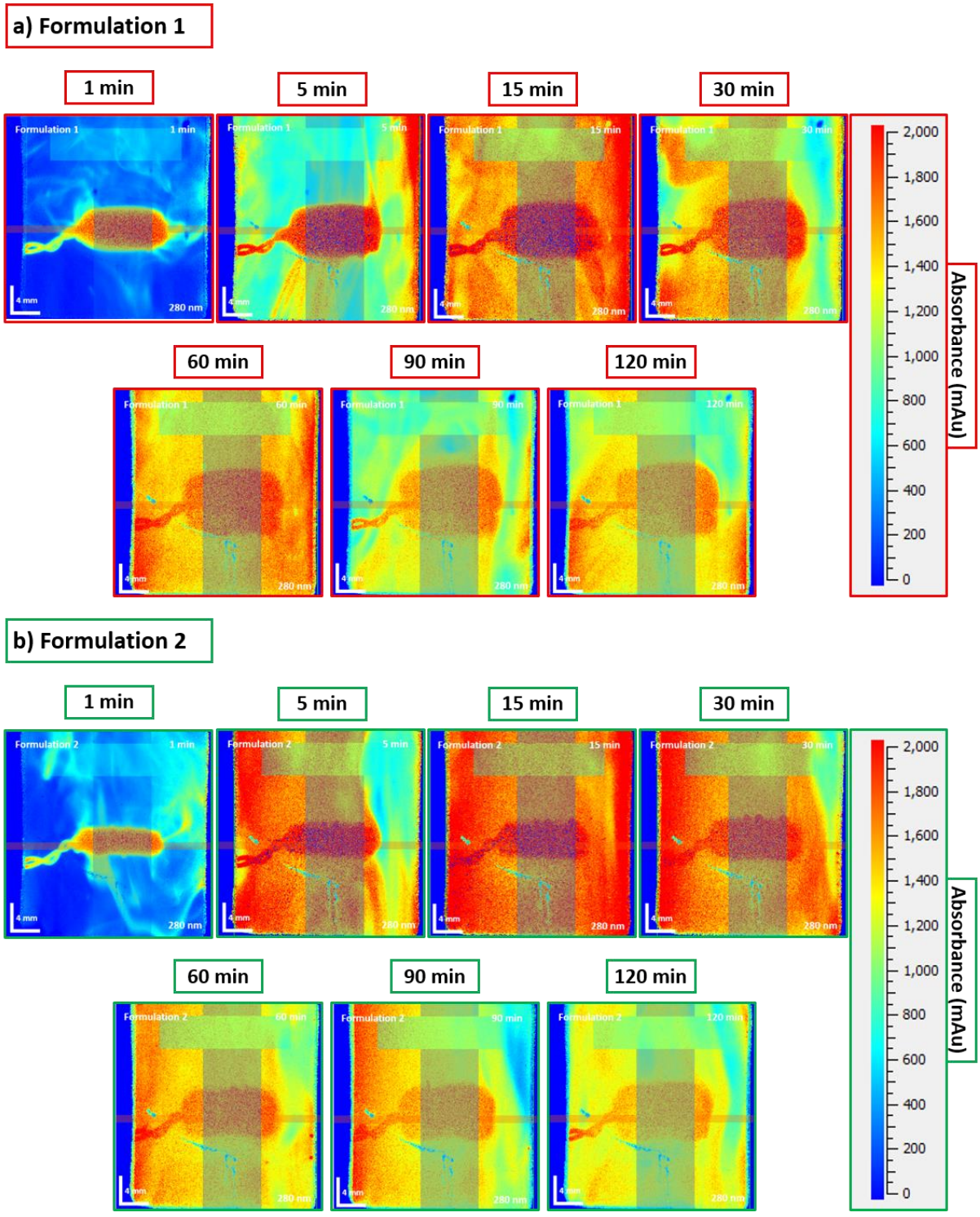
a) Formulation 1
1 min
5 min
15 min
30 min
60 min
90 min
120 min
Absorbance (mAu)
2,000
1,800
1,600
1,400
1,200
1,000
800
600
400
200
0
b) Formulation 2
1 min
5 min
15 min
30 min
60 min
90 min
120 min
Absorbance (mAu)
2,000
1,800
1,600
1,400
1,200
1,000
800
600
400
200
0

Figure 5

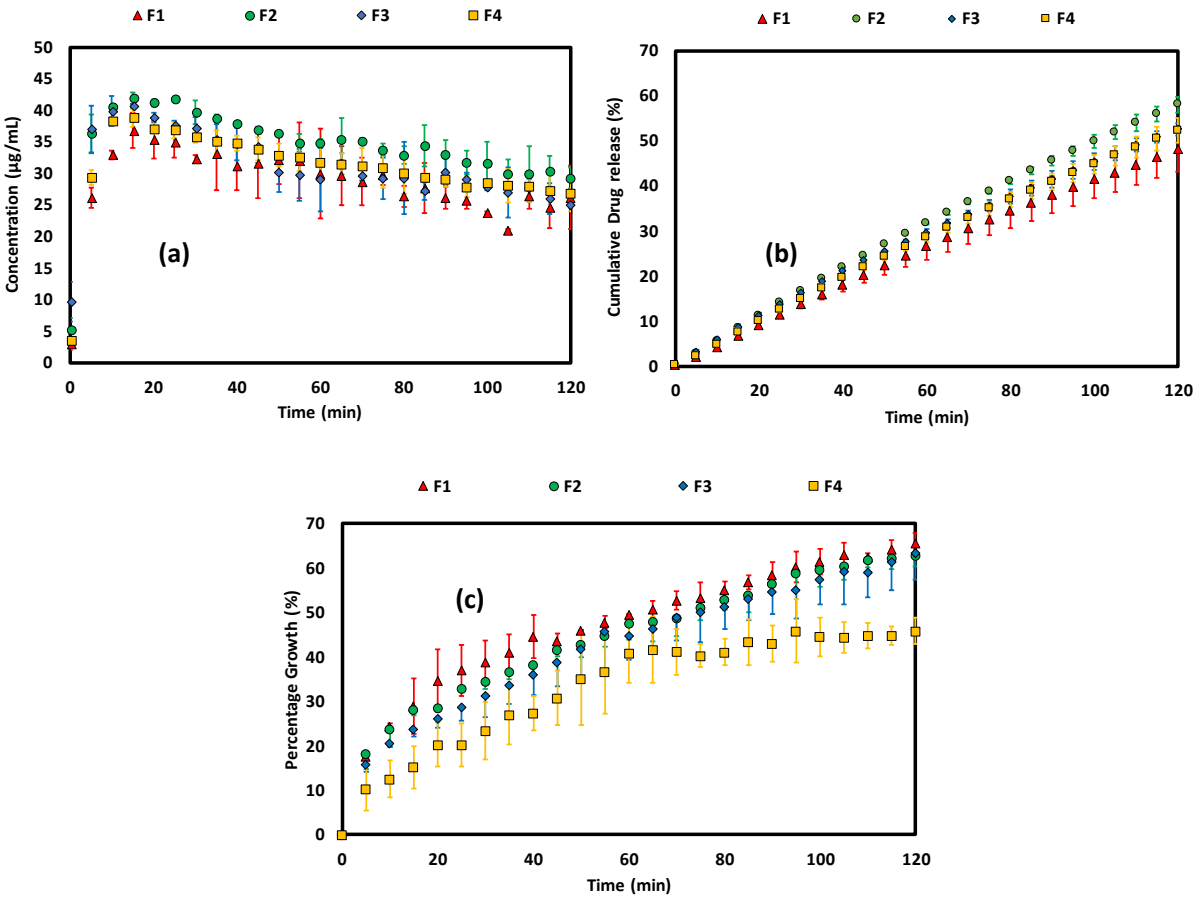

584

585

586 **Figure 6**

587

588

589

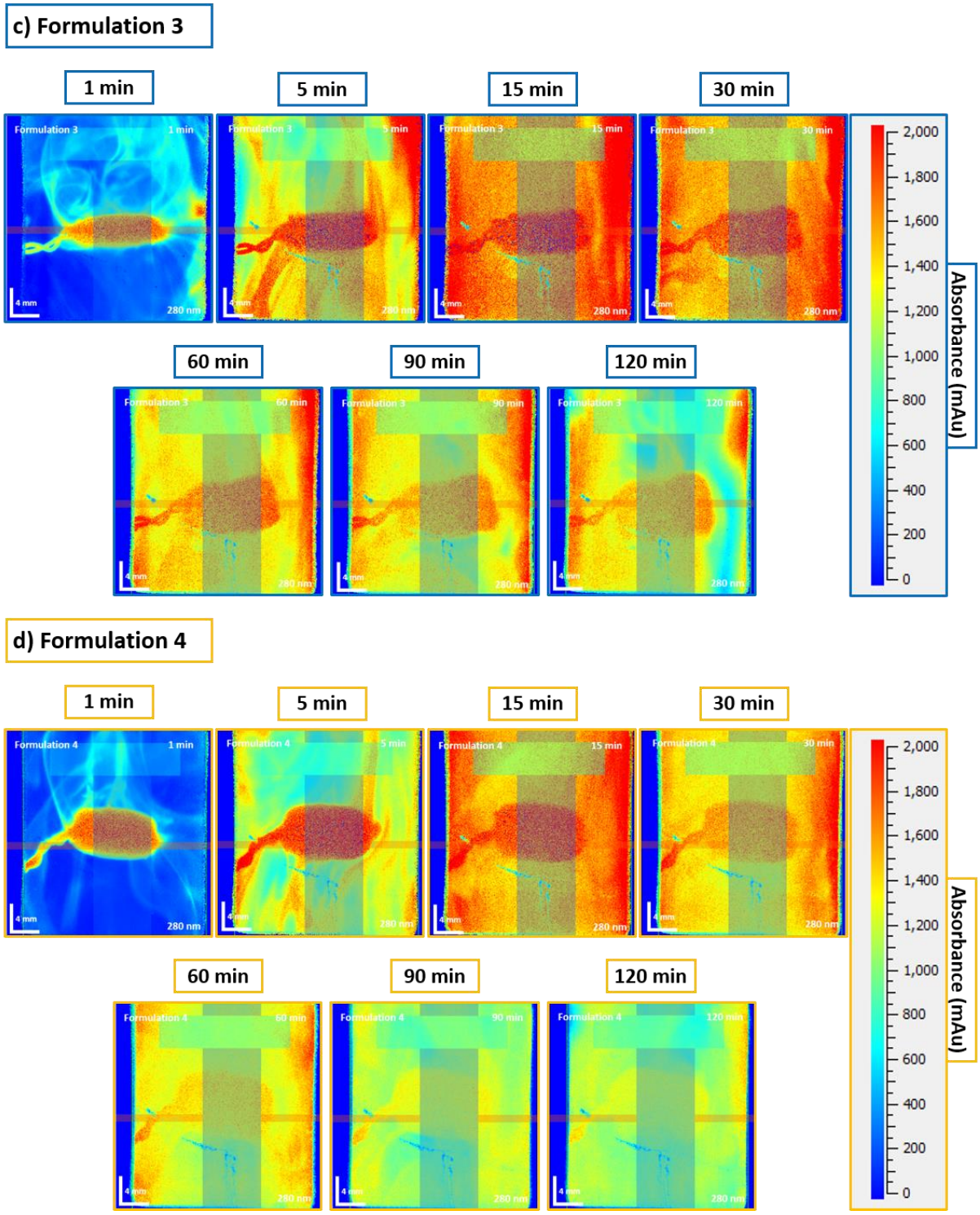
c) Formulation 3
1 min
5 min
15 min
30 min
60 min
90 min
120 min
Absorbance (mAu)
2,000
1,800
1,600
1,400
1,200
1,000
800
600
400
200
0
d) Formulation 4
1 min
5 min
15 min
30 min
60 min
90 min
120 min
Absorbance (mAu)
2,000
1,800
1,600
1,400
1,200
1,000
800
600
400
200
0

Figure 7